



DOI: [10.29026/oea.2022.210121](https://doi.org/10.29026/oea.2022.210121)

# Label-free trace detection of bio-molecules by liquid-interface assisted surface-enhanced raman scattering using a microfluidic chip

Shi Bai<sup>1</sup>, Xueli Ren<sup>2</sup>, Kotaro Obata<sup>1</sup>, Yoshihiro Ito<sup>2</sup> and Koji Sugioka<sup>1\*</sup>

<sup>1</sup>Advanced Laser Processing Research Team, RIKEN Center for Advanced Photonics, RIKEN, 2-1 Hirosawa, Wako, Saitama 351-0198, Japan;

<sup>2</sup>Nano Medical Engineering Laboratory, RIKEN Cluster for Pioneering Research, 2-1 Hirosawa, Wako, Saitama 351-0198, Japan.

\*Correspondence: K Sugioka, E-mail: ksugioka@riken.jp

Supplementary information for this paper is available at <https://doi.org/10.29026/oea.2022.210121>



Open Access This article is licensed under a Creative Commons Attribution 4.0 International License.

To view a copy of this license, visit <http://creativecommons.org/licenses/by/4.0/>.

© The Author(s) 2022. Published by Institute of Optics and Electronics, Chinese Academy of Sciences.

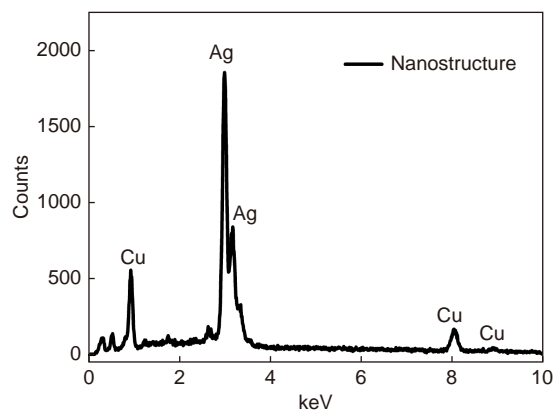


**Fig. S1 | EDS spectra of 2-D Ag-Cu nanostructure fabricated by LIPSS.**

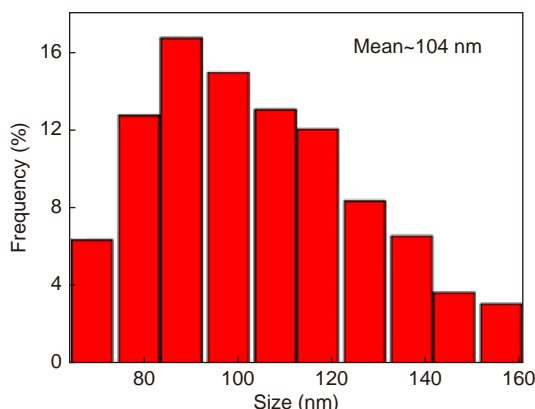


**Fig. S2 | Size distribution of metal nanodots fabricated by two-step laser scanning.** The mean size is about 104 nm with a standard deviation of 29 nm.

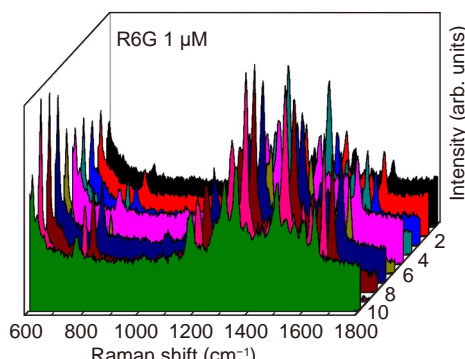


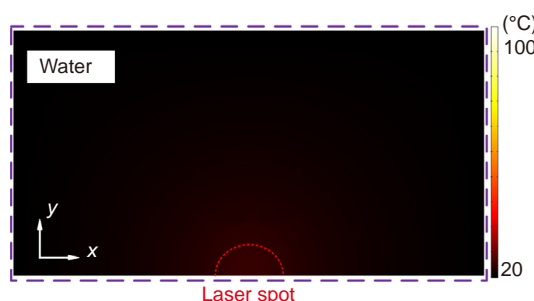
**Fig. S3 | SERS spectra of 1 μM R6G solution using ten microfluidic SERS chips.** The relative standard deviation of AEF calculated based on the ten spectra was 10.1% (at 604 cm⁻¹).

**Table S1 | Relative standard deviation (RSD) of the main Raman peaks of R6G (1 μM).**

Raman peak (cm⁻¹)	RSD (%)
604	10.1
765	9.2
1177	8.9
1305	13.5
1354	16.2
1502	14.5
Average	11.7

**Table S2 | The DNA sequence for LI-SERS measurements used in Figure 5(a).**

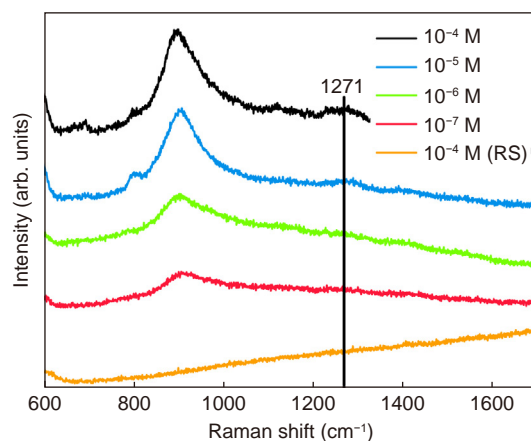
Sequence	A	T	C	G
TATAAATACAAGTACCATCAGGCAGAACACAAACAGCATAAG (42 mer)	50% (21 mer)	14.29% (6 mer)	21.43% (9 mer)	14.29% (6 mer)

**Fig. S4 | Simulation of the fluid temperature in the liquid on the SERS substrate.** The laser beam irradiates into the liquid and the initial temperature is 20 °C.**Table S3 | DNA sequences for discrimination used in Figure 5(b).**

Sequence	A	T	C	G
S1:TCCACAAACCATGTCCTGATAGTTTCAGC (30 mer)	23.33% (7 mer)	33.33% (10 mer)	30% (9 mer)	13.33% (4 mer)
S2:TAAATACAAGTACCATCAGGCAGAACACAAACAGC (35 mer)	48.57% (21 mer)	11.43% (6 mer)	25.71% (9 mer)	14.29% (6 mer)

**Table S4 | Recently developed SERS platforms for the trace detection of Aβ.**

SERS platform	Capping agents/Linker	Detection limit	Ref.
Au nanoshell	Sialic acid	1 pM	1
Hollow Au/Ag nanostar	Thioflavin	10 nM	2
Au nanoparticle	Anti-Aβ antibody	1 μM	3
Au nanoparticle	Rose Bengal	2 μM	4
Ag nanogap shell	Aβ antibody	55 fM	5
Graphene oxide - gold shell nanoparticle	Aβ antibody	22 fM	6
Au nanoparticle	Label-free	70 pM	7
3D Au nanowire array	Label-free	1 nM	8
Au nanoparticle in nanochannel	Label-free	10 pM	9
Ag-Cu nanostructure in microchannel	Label-free	<1 pM	Present work

**Fig. S5 | Raman spectra of Aβ (29-40) measured by the regular SERS method for different concentrations ( $10^{-4}$  M to  $10^{-7}$  M) and Raman spectroscopy (RS) on glass surface for  $10^{-4}$  M.**

## References

- S1. Beier HT, Cowan CB, Chou IH, Pallikal J, Henry JE et al. Application of surface-enhanced Raman spectroscopy for detection of beta amyloid using nanoshells. *Plasmonics* **2**, 55–64 (2007).
- S2. Garcia-Leis A, Torreggiani A, Garcia-Ramos JV, Sanchez-Cortes S. Hollow Au/Ag nanostars displaying broad plasmonic resonance and high surface-enhanced Raman sensitivity. *Nanoscale* **7**, 13629–13637 (2015).
- S3. Credi C, Bibikova O, Dallari C, Tiribilli B, Ratto F et al. Fiber-cap biosensors for SERS analysis of liquid samples. *J Mater Chem B* **8**, 1629–1639 (2020).
- S4. Xia Y, Padmanabhan P, Sarangapani S, Gulyás B, Matham MV. Bifunctional fluorescent/Raman nanoprobe for the early detection of amyloid. *Sci Rep* **9**, 8497 (2019).
- S5. Yang JK, Hwang IJ, Cha MG, Kim HI, Yim DB et al. Reaction kinetics-mediated control over silver nanogap shells as surface-enhanced Raman scattering nanoprobes for detection of Alzheimer's disease biomarkers. *Small* **15**, 1900613 (2019).
- S6. Demeritte T, Nellore BPV, Kanchanapally R, Sinha SS, Pramanik A et al. Hybrid graphene oxide based plasmonic-magnetic multifunctional nanoplateform for selective separation and label-free identification of Alzheimer's disease biomarkers. *ACS Appl Mater Interfaces* **7**, 13693–13700 (2015).
- S7. Zhou Y, Liu J, Zheng TT, Tian Y. Label-free SERS strategy for in situ monitoring and real-time imaging of A $\beta$  aggregation process in live neurons and Brain Tissues. *Anal Chem* **92**, 5910–5920 (2020).
- S8. Lin DD, Wu ZL, Li SJ, Zhao WQ, Ma CJ et al. Large-area Au-nanoparticle-functionalized Si nanorod arrays for spatially uniform surface-enhanced Raman spectroscopy. *ACS Nano* **11**, 1478–1487 (2017).
- S9. Chou IH, Benford M, Beier HT, Coté GL, Wang M et al. Nanofluidic biosensing for  $\beta$ -amyloid detection using surface enhanced raman spectroscopy. *Nano Lett* **8**, 1729–1735 (2008).